TU/e EINDHOVEN UNIVERSITY OF TECHNOLOGY

Active noise control of an acoustic duct using feedback control

Citation for published version (APA):
Boot, J. (2004). *Active noise control of an acoustic duct using feedback control*. (DCT rapporten; Vol. 2004.042). Technische Universiteit Eindhoven.

Document status and date:
Published: 01/01/2004

Document Version:
Publisher's PDF, also known as Version of Record (includes final page, issue and volume numbers)

Please check the document version of this publication:

• A submitted manuscript is the version of the article upon submission and before peer-review. There can be important differences between the submitted version and the official published version of record. People interested in the research are advised to contact the author for the final version of the publication, or visit the DOI to the publisher's website.
• The final author version and the galley proof are versions of the publication after peer review.
• The final published version features the final layout of the paper including the volume, issue and page numbers.

Link to publication

General rights
Copyright and moral rights for the publications made accessible in the public portal are retained by the authors and/or other copyright owners and it is a condition of accessing publications that users recognise and abide by the legal requirements associated with these rights.

• Users may download and print one copy of any publication from the public portal for the purpose of private study or research.
• You may not further distribute the material or use it for any profit-making activity or commercial gain
• You may freely distribute the URL identifying the publication in the public portal.

If the publication is distributed under the terms of Article 25fa of the Dutch Copyright Act, indicated by the "Taverne" license above, please follow below link for the End User Agreement:

www.tue.nl/taverne

Take down policy
If you believe that this document breaches copyright please contact us at:

openaccess@tue.nl

providing details and we will investigate your claim.

Download date: 16. Nov. 2023

Active noise control of an acoustic duct using feedback control

Johan Boot
Report number 2004.42

San Diego, U.S.A,
Februari 20, 2004

Advisor: Raymond A. de Callafon
University of Califonia, San Diego
Department om Mechanical and Aerospace engineering

University of Technology, Eindhoven
Department of Mechanical Engineering,
Control Systems Technology

Abstract

Forced air cooling systems, such as an airconditioning system produce noise. For a pleasant living environment, this noise is undesirable. A way to suppress produced noise is reducing the sound in the duct where the air flows through afterwards. This report handles the noise reduction in an active duct silencer by the use of a discrete feedback controller. Models of the involved processes are made. With these models and suitable choices of weighting functions, an H_2 optimal controller is calculated. The controller is reduced taking into account the sensitivity of the closed loop process. Stability and performance are maintained in this way. Finally the controller is implemented on the system and a validation has been made to indicate the active noise cancellation that could be obtained with feedback control.

Contents

Introduction

Most modern buildings are equipped with air conditioning systems. A central unit handles fresh air which flows true a number of ducts to the rooms where people reside. Besides the fresh heated or cooled air, the air treatment system also produces noise due to the forced flow of air. For a pleasant environment, the noise should be reduced to a comfortable level.

In current situations, the noise is reduced to a lower level by changing a part of the duct by a passive silencer duct. This is a duct which passively absorbs the energy of the sound waves by the means of using the right shape and additional damping material [1, Tang]. An idea for improving the performance of this duct is done by adding a microphone-speaker combination in the duct. The microphone which is located in the beginning of the duct measures the noise so the loudspeaker located further in the duct can compensate this noise by sending an inverse sound of the original noise. This is also called noise cancellation by feed-forward control. This way of improving the silencer is very efficient and significant results are obtained between frequencies of 40 and 400 Hertz [2, Zeng].

An other idea of improving the silencer is locating the microphone closely behind the speaker and then trying to reduce the sound waves at that point as much as possible. This kind of control is called feedback control [3, Hull],[4, Hong]. In this report the possibilities of feedback control in an active duct silencer will be explored.

Chapter 1

Objectives and problem definition

The objective of this report is to explore the possibilities of noise reduction in a acoustic duct using feedback control techniques that cancel sound using a microphone in the downstream location of the acoustic duct.

To achieve this goal, the following problems have to be solved.

- The dynamic sound propagation through the duct has te be modelled. This can be done based on physics based modelling or experimental system identification. Practice has to reveal which method is preferable.
- A low order optimal controller has to be designed. H_2 optimization and subsequently system reduction is suitable to reach these goals. During the reduction of the controller, the stability of the closed system should not be left aside.
- For implementation, an evaluation of minimal sampling frequency for digital control is needed. The final design will be examined and discussed.

Chapter 2

Description of experimental apparatus

2.1 Acoustic duct arrangement

The system which will be analyzed is an ACTA air ventilation silencer duct located in the Systems Identification and Control Laboratory (SICL) at the University of California, San Diego. The right side of the duct is connected to an approximately two meters long tube with a bend of 90^o in it. At the end, a loudspeaker is mounted which can produce a noise to simulate a forced airflow system. From now on this speaker will be defined as the 'disturbance speaker'. The left end of the duct is open and also the microphone is fixed on this place. For about thirty centimeters of the microphone, the control speaker, or just 'speaker' is located. For the amplification of the signals, amplifiers with a constant gain are used. In the frequency region from $25Hz$ to $5kHz$, these amplifiers amplify linear without significant dynamical deviations. When there will be spoken about the input or output signals, there is referred to the voltages going in or out the physical system without the amplifiers. In this way no confusion can come into being from changing the gains of the amplifiers. A siglab system and DSP-card are present for analyses and controller implementation. Matlab is used for calculations.

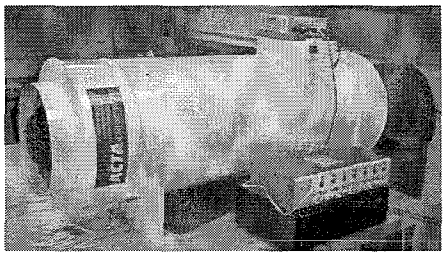

Figure 2.1: Silencer duct

2.2 Schematic view of the duct

For control purposes, it is convenient to make a scheme of the system. In figure 2.2 the system is represented schematically. The input signal to the control speaker is denoted by u. The final noise signal at the microphone at the end of the duct is denoted by y. The relation between these two signals is the dynamic transfer function G. The disturbance signal at the point of the microphone is denoted by d. The spectrum of d can always be characterized by a filtered white noise. For that purpose we define that d is the product of H and n, where H is a stable and stable invertible filter. The filter H is also called the disturbance model.

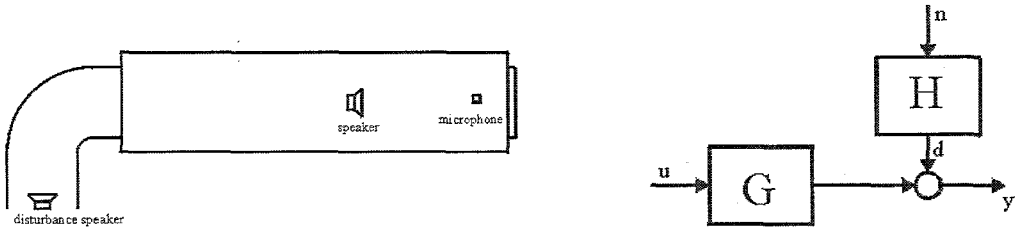

Figure 2.2: Scheme of the silencer duct

When a feedback controller would be implemented between the output signal y and the input of the speaker u, the dynamics of G and H are critical for performance limitations. The dynamics of G are in particular important because they are also critical for stability of the final closed loop system. To give an indication of the dynamics of G, the frequency response between the signals y and u is measured and showed in figure 2.3.

According to the coherence of the frequency response at frequencies above 50 Hz, a linear model of the process G is a good assumption. In contrary to most mechanical systems, the magnitude of the frequency response does not decreases with higher frequencies in the interesting frequency range. However the phase decreases rapidly with higher frequencies. The shape of the phase indicates a pure time delay. This definitely makes sense because of

the character of sound waves. Sound waves transport themselves with a speed of approximately 340 m/s. When the sound has to overcome the distance from the speaker to the microphone, a certain time will elapse.

In the case of a pure phase delay, the phase revolution can be calculated as follows:

$$phase \quad revolution = \frac{360\ f\ \delta x}{c} \tag{2.1}$$

This is applied to the frequency response data with the assumption, that there is only a pure time delay. Now it follows that the microphone and speaker are located 29 centimeters apart. This distance is verified by a correlation measurement.

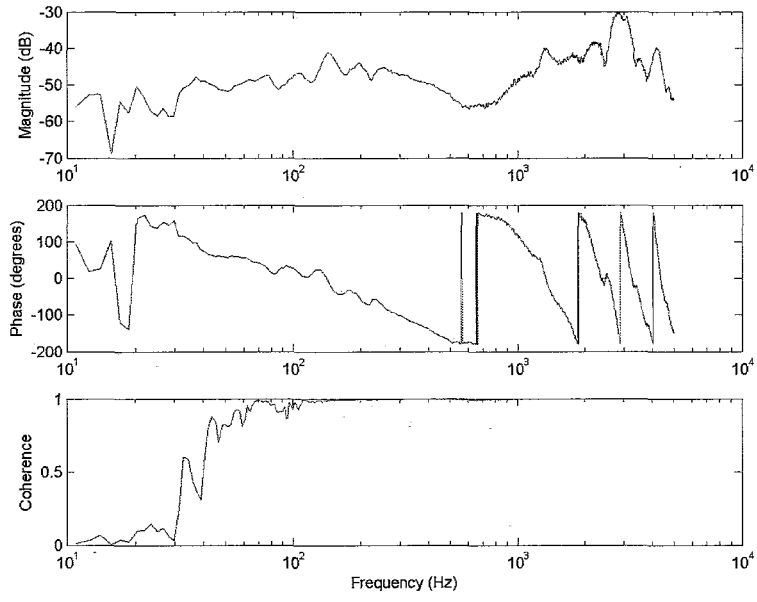

Figure 2.3: Frequency response of process G

Chapter 3

Theoretical modelling

3.1 Acoustic model

To obtain a good understanding of the properties of the system, a theoretical analysis is a done. For a simplified model, the duct is considered as an one end opened 1-D duct filled with an ideal gas [4, Hong]. To analyse this system, a small volume element is considered. For such a volume element, the equation of state, the equation of continuity and Euler's force equation must apply. After a number of mathematical transactions and the inclusion of proportional damping, an continuous equation is obtained. When this is transformed to the state-space notation, a number of higher harmonics of the natural eigenfrequency has to be chosen which determines the order of the model. Here the input is the speed of the speaker baffle, and the output is the pressure at the microphone.

$$\begin{aligned} \dot{x}_d(t) &= A_d x_d(t) + B_d u_x(t), \\ y_d(t) &= C_d x_d(t) \end{aligned} \tag{3.1}$$

where:

$$\begin{aligned} A_d &= diag\left(\begin{bmatrix} 0 & 1 \\ -\omega_{n1}^2 & -2\zeta_1\omega_{n1} \end{bmatrix}, \quad \cdots \quad, \begin{bmatrix} 0 & 1 \\ -\omega_{nr}^2 & -2\zeta_r\omega_{nr} \end{bmatrix}\right) \\ B_d &= [0 \quad V_1(x_m) \quad \ldots \quad 0 \quad V_r(x_m)]^T \\ C_d &= [V_1(x_s) \quad 0 \quad \ldots \quad V_r(x_s) \quad 0] \\ D_d &= [0] \end{aligned} \tag{3.2}$$

and:

$$w_i = \tfrac{i\pi c}{L} \tag{3.3}$$

$$V_i(x) = c\sqrt{\tfrac{2}{L}}\sin k_i x \tag{3.4}$$

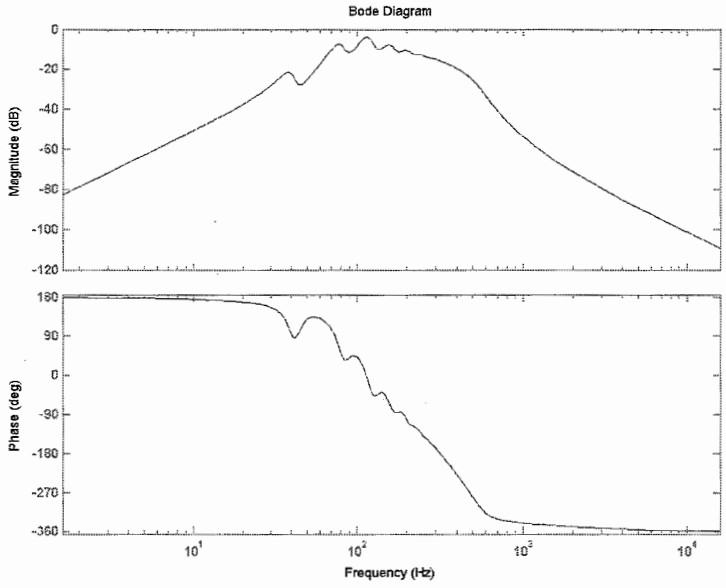

Figure 3.1: Frequency response of the model

When looking at the frequency response function of this model, similarities with the real system definitely can be seen. Unfortunately this model is not suitable for real modelling of the duct because of the following main reasons.

- The duct is not just an open-open tube. At the end there starts another piece of pipe with an 90^o angle in it. So there are many places to reflect the sound and a lot of different harmonics will exists.
- In reality the sound waves travel in all three dimensions and not just in one dimension like one of the assumptions.
- No good estimation of damping and boundary layers can be made with this simple model.

3.2 Lumped mass model

Another model which gives a good impression of the physics of the system is a lumped mass model. The duct is divided in a number of volume elements in longitudinal direction. Each of these elements can be seen as an element with a mass and a stiffness. The model consists only of a number of masses and springs in series. The calculations of the spring stiffness and the mass is quite easy and depends on the number of volume elements of the duct. Open or closed boundary conditions for the ends can be chosen by having springs at the end of the series of masses or not. The force applied by the speaker can be applied to one of the masses. The pressure difference at the microphone can be seen as the difference in distance between two volume elements which represents an compressed spring or compressed air.

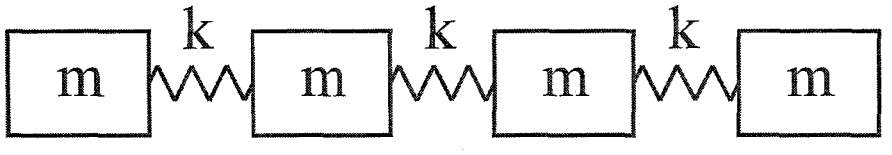

Figure 3.2: Lumped mass model

This representation of the system gives a clear comparison with a mechanical system. When the microphone is a lot of volume elements widened of the speaker, it looks natural that there is more decay in phase at higher frequencies. The performance of the controlled system will be limited.

When this model is used with enough volume elements, the similary with the preceding model is large. For the same reasons as shown in the preceding section, this model gives a good insight in the model physics, but is not suitable for modelling. The real system is just too complex to make do a valid modelling based on the system knowledge. Therefore, in the next chapter a modelling will be discussed with no prior model knowledge. Or in other words with a black box approach.

Chapter 4

Experimental modelling

4.1 Linear regression model

Because the dynamics of G will be enclosed in the controller loop, it is critical for stability. For this reason it is important to model the dynamics accurate. G will be modelled as a discrete time-invariant linear system. First of all a high order model will be estimated. Later can be decided if there exists the need for a reduction of this model. When not used for controller design, a high order model is still convenient for validation of the final controller.

A good way to estimate a high order model is using the linear regression or ARX model structure [5, Ljung]. The ARX model structure describes the system with the following linear difference equation:

$$y(t) + a_1 y(t-1) + ... + a_{n_a} y(t-n_a) = b_1 u(t-1) + ... + b_{n_b} u(t-n_b) + e(t) \qquad (4.1)$$

For the calculation of the next output $y(t)$, a lineair combination of outputs $y(t)$ in history and a linear combination of inputs $u(t)$ in history is used. In the linear regression model, the effect of noise is modelled as an equation noise, that directly acts as a white noise disturbance on the current output. An important note is to mention that the signal $e(t)$ of the system above does not correspond to the signal $n(t)$ of the duct. The reason why they don't correspond with each other is that during the measurement on the duct, the noise $n(t)$ will not be present at all to get better measurement data. The noise $e(t)$ will only represent model and measurement errors.

A more compact notation can be used for the same difference equation. A depiction of the signals with the use of an alternate notation is used in figure 4.1.

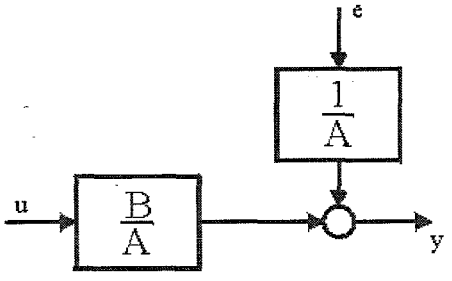

Figure 4.1: The ARX model structure

$$y(t) = \frac{B(q)}{A(q)}u(t) + \frac{1}{A(q)}e(t) \tag{4.2}$$

with $A(q)$ and $B(q)$

$$A(q) = 1 + a_1 q^{-1} + ... + a_{n_a} q^{-n_a} \tag{4.3}$$
$$B(q) = b_1 q^{-1} + ... + b_{n_b} q^{-n_b} \tag{4.4}$$

and the parameters of the system can be summarized in θ, where

$$\theta = [a_1 \ a_2 \ ... \ a_{n_a} \ b_1 \ ... \ b_{n_b}]^T \tag{4.5}$$

The contribution of the error signal in the output exists of the error which is filtered by the denominator dynamics of the plant. This is not corresponding with reality and gives a unnatural representation. In reality the error describes modelling and measurement errors. The reason this method still is favorable, is that the predictor uses a linear regression.

$$\hat{y}(t|\theta) = B(q)u(t) + [1 - A(q)]y(t) \tag{4.6}$$

With the introduction of the known vector of past data

$$\varphi = [-y(t-1) \ ... \ -y(t-n_a) \ u(t-1) \ ... \ u(t-n_b)]^T \tag{4.7}$$

equation 4.6 can now become very simple.

$$\hat{y}(t|\theta) = \varphi^T(t)\theta \tag{4.8}$$

When this prediction model is compared with the real measured data, the prediction error is given by

$$\varepsilon(t,\theta) = y(t) - \hat{y}(t|\theta) = y(t) - \varphi^T(t)\theta \tag{4.9}$$

For minimizing this linear equation with many parameters and a lot of data points, numerical solutions are available. When a closer look on ε is taken, there can be seen that actually the following is minimized.

$$\varepsilon(t,\theta) = A(q)\left(y(t) - \frac{B(q)}{A(q)}u(t)\right) \tag{4.10}$$

When both the input $u(t)$ and output $y(t)$ data is pre-filtered by a frequency weighing filter $L(q)$ it changes epsilon in the following way.

$$\varepsilon(t,\theta) = A(q)L(q)\left(y(t) - \frac{B(q)}{A(q)}u(t)\right) \tag{4.11}$$

Thus can be concluded that a weighing filter has the same effect as the inverse of the noise model. The noise model of an ARX model is the denominator of the process. The frequency response of the inverse of the denominator of the process increases quickly with higher frequencies. A specific characteristic of the ARX estimation is that it is most accurate for high frequencies.

Results

In the modelling phase the signals are pre filtered by a filter. This filter contains a low pass component which looks like the denominator of the estimated process. In this way the focussing on the higher frequencies is for the greater part undone. Also it contains a filter which focusses on the interesting region.

The data is sampled at 2.56 kHz and a model is made with a enumerator polynomial of order 50 and a denominator polynomial of order 50. When the system is modelled at a higher order or with a higher frequency range, the denominator process will have a larger amplitude region. When the pre-filter has to compensate for this, a very strong suppression of the high frequent data will me made. When the model order or the frequency range are chosen too high, the pre-filtering causes such low power of the signals at high frequencies which introduce singularities in the calculations. In figure 4.2, a frequency response of the real system and the model are plotted.

In the region between 50 and 500 Hz, a good fit is obtained. At the lower frequencies, nothing sensible can be said about the fit, because of the low coherence of the original measurement. At the highest frequencies a bad result is obtained because of the high suppression of high frequencies by the pre-filtering.

The model is now decomposed in zeros and poles. All the high and low frequent poles and zeros are thrown away. This results in a model of order 18. Also, the model is re-sampled to a frequency of 5.12 kHz by a discrete to continuous conversion and a back conversion on the new sample rate. The model is not suitable to represent the system, but can be used for a next step.

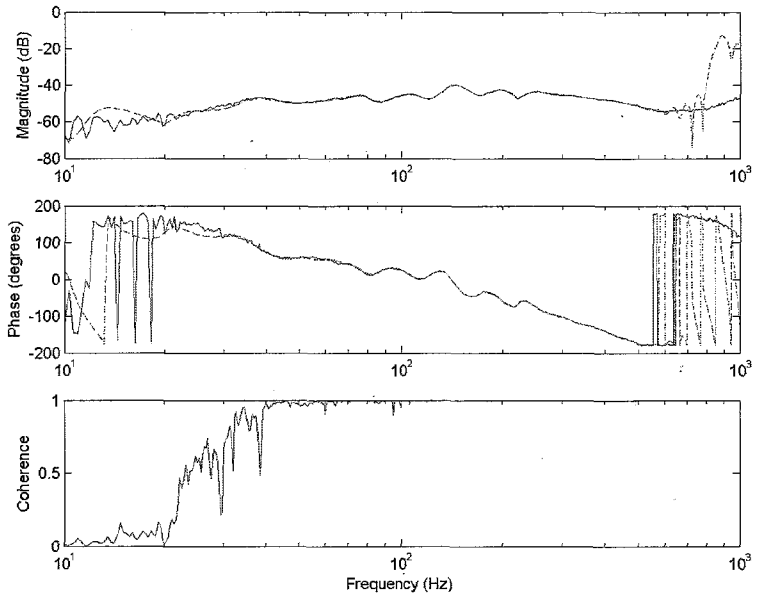

Figure 4.2: Frequency response of process G (solid) and the ARX-modelled system (dashed)

4.2 Output error model

In the output error (OE) model structure, the white noise does not directly involve the states, but only influences the output directly. From the physical point of view this is much more logic.

$$w(t) + f_1 w(t-1) + ... + f_{n_f} w(t-n_f) = b_1 u(t-1) + ... + b_{n_b} u(t-n_b) \tag{4.12}$$

$$y(t) = w(t) + e(t) \tag{4.13}$$

Again, this can be rewritten in a more practical notation which gives a direct perception of the noise directly influencing the output.

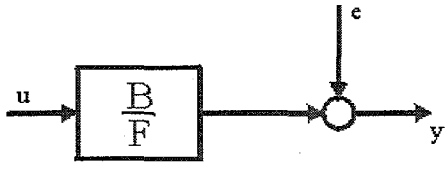

Figure 4.3: The OE model structure

$$y(t) = \frac{B(q)}{F(q)}u(t) + e(t) \tag{4.14}$$

with $A(q)$ and $F(q)$

$$A(q) = 1 + f_1 q^{-1} + ... + f_{n_f} q^{-n_f} \tag{4.15}$$

$$B(q) = b_1 q^{-1} + ... + b_{n_b} q^{-n_b} \tag{4.16}$$

and the parameters of the system

$$\theta = [b_1\ b_2\ ...\ b_{n_b}\ f_1\ f_2 ...\ f_{n_f}]^T, \tag{4.17}$$

This model gives a better representation of reality than the ARX model. The problem involved with this model can be seen when looking at the predictor.

$$\hat{y}(t|\theta) = \frac{B(q)}{F(q)}u(t) = w(t,\theta) \tag{4.18}$$

With the known vector of past data

$$\varphi(t,\theta) = [u(t-1)\ ...\ u(t-n_b)\ -w(t-1,\theta)\ ...\ -w(t-n_f,\theta)]^T \tag{4.19}$$

equation 4.18 can now become very simple.

$$\hat{y}(t|\theta) = \varphi^T(t,\theta)\theta \tag{4.20}$$

In equation 4.19, the $w(t-1,\theta)$ are not directly measured. They can still be calculated by equation 4.18. These are actually the old estimates of $y(t)$ which are calculated using the parameters θ. This makes 4.20 no longer linear, but a pseudo linear function. For minimizing the error by finding the right parameters θ, iteration steps are required. This type of modelling is suitable for models with not too much parameters. In this way, large calculation times are avoided, and a higher chance is obtained of finding the global optimum.

Results

Data, sampled at 5.12 kHz is used for modelling. First of all, the output data is filtered by the inverse of the found and simplified ARX-model. In this way, al the dynamics already modelled by the ARX-model are removed. The resulting dynamics mainly consists of the higher frequent components which were not modelled by the first model. A tenth order numerator and denominator are estimated. This model is multiplied with the first model and now a 28th. order model is obtained. When the frequency response of the model is compared with the measured frequency response in figure 4.4, a nice similarity is seen. When comparing real data and simulated data in figure 4.5, this also gives some confidence in the model.

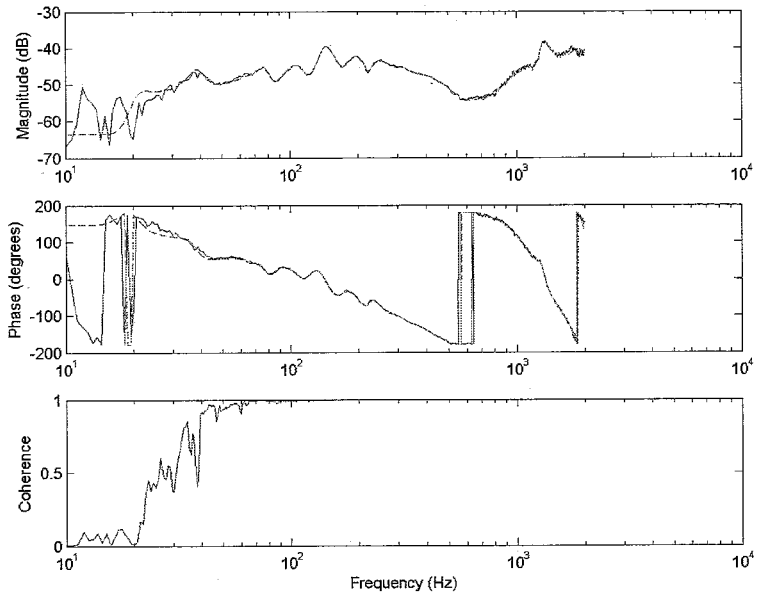

Figure 4.4: Frequency response of process G (solid) and the final modelled system (dashed)

4.3 Noise modelling

For the controller design, some other models are required. For example the model H, which describes the noise source is required. The noise models found in above sections do not correspond with H. This because the noise source was turned off during measurements for a better determination of G. Besides, the two methods used for the noise models are not suitable for determination of H. In the ARX method, an $H(\theta) = 1/A(\theta)$ was found and in the OE method, $H(\theta) = 1$ was found. Therefore, in the OE model, an extra estimate of the noise model must be made.

These models are only used as a weighing function and are therefore not critical for stability. There is chosen to model these systems by placement of zeros and poles. In this way it is very easy to keep an eye on the order of the models. There is no need for an exact representation of the systems, just in the interesting regions, the amplitude must be right. The order of the models must be as small as possible, because they also increase the order of the controller.

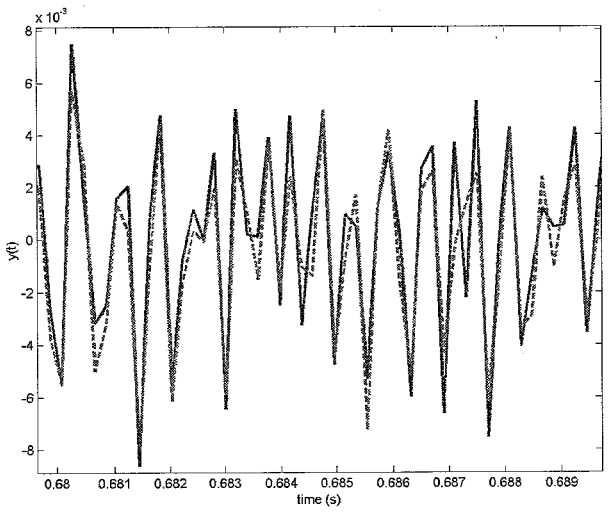

Figure 4.5: Experimental data of $y(t)$ (solid) and simulations (dashed)

Conclusion

With the use of experimental modelling, a 28^{th} order model is found which represents the physical system G well with simulations and in the frequency domain. For the noise source H, a 8^{th} order model is made on the base of pole/zero placement.

Chapter 5

Controller design

5.1 H_2 optimal design

To obtain clear objectives for the controlled system, the H_2 approach is used [6, Sima], [7, Saberi]. For this method, the system will be written in the augmented standard plant form P.

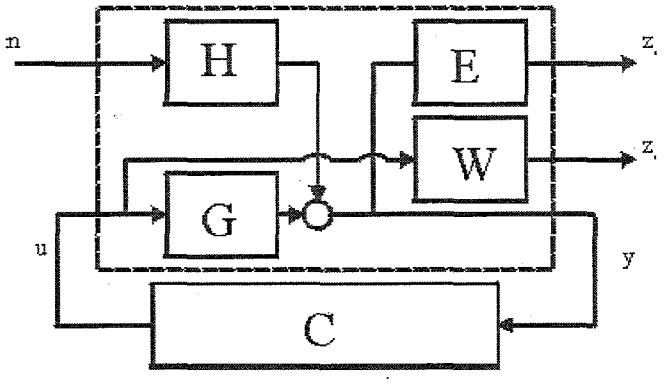

Figure 5.1: Augmented standard plant P in closed loop

The augmented plant has two inputs. The input n is an unity random white noise. When this noise is filtered through filter H, the noise at the error microphone is formed. At input u, the control action will interact with the system. When this signal is filtered through the process G, it represents the control action at the position of the error microphone. When these two signals are summed, they represent the whole output signal y.

The output signals of the system contains of two groups. The signals z_1 and z_2 are in the same group and are desired to be as small as possible. Signal z_1 resembles the output signal which is logically preferred to be as small as possible. The multiplication with the filter E gives accents in which frequency regions the ear is most sensible and the noise is therefore most undesired. The output z_2 wants to give some restrictions to the controller C. To accomplish that, the signal u has to be weighted with the inverse of the process H and filtered by another filter which enforces the regions where no control action of the controller C is desired.

In this situation, the standard plant is described by the 2 input, three output transfer function P and the 1 input, 2 output closed loop transfer function P_{cl}

$$\begin{bmatrix} z_1(t) \\ z_2(t) \\ y(t) \end{bmatrix} = P(q) \begin{bmatrix} n(t) \\ u(t) \end{bmatrix}, \quad \begin{bmatrix} z_1(t) \\ z_2(t) \end{bmatrix} = P_{cl}(q,\theta)n(t), \quad \begin{bmatrix} z_1(t) \\ z_2(t) \end{bmatrix} = z(t) \tag{5.1}$$

where

$$P(q) = \begin{bmatrix} HE & GE \\ 0 & W \\ H & G \end{bmatrix}, \quad P_{cl}(q,\theta) = \begin{bmatrix} \frac{HE}{1+CG} \\ \frac{HCW}{1+CG} \end{bmatrix} \tag{5.2}$$

The H_2 method minimizes the RMS value of the output $z(t)$ of the standard plant as an function parameters θ of the controller $C(q,\theta)$. Minimizing the RMS values of the output $z(t)$ is equivalent with minimizing the following:

$$\begin{aligned} \|z(t)\|_{RMS} &= \left(\lim_{K\to\infty} \frac{1}{K} \sum_{t=0}^{K} z_1^2(t) + z_2^2(t) \right)^{1/2} \\ &= \left(\lim_{K\to\infty} \frac{1}{K} \sum_{t=0}^{K} z(t)'z(t) \right)^{1/2} = \left(\frac{1}{2\pi} tr \left[\int_{-\pi}^{\pi} S_z(\omega) d\omega \right] \right)^{1/2} \end{aligned}$$

where the power spectral density $S_z(\omega)$ of $z(t)$ is a function of the power spectral density $S_n(\omega)$ of the stationary stochastic input $n(t)$

$$S_z(\omega) = P_{cl}(e^{j\omega}) S_n(\omega) P_{cl}'(e^{-j\omega}), \quad -\pi \leq \omega \leq \pi \tag{5.3}$$

If the system is excited by a stochastic zero mean white noise with a variance of one, the H_2 norm of $P_{cl}(q,\theta)$ is equivalent with the RMS-value of the output $z(t)$. Since the output $z(t)$ has to be minimized, this is equivalent by minimizing the 2-norm of P_{cl}.

$$\min_{\theta} \|P_{cl}(q,\theta)\|_2 = \min_{\theta} \left\| \left[\frac{H(q)E(q)}{1+C(q,\theta)G(q)} \quad \frac{H(q)C(q)W(q)}{1+C(q,\theta)G(q)} \right]^T \right\|_2 \tag{5.4}$$

To solve this minimization, Ricatti equations, analogous to the ones in the LQG design, have to be solved. Elaborating on the analogy, the weighting functions used in the LQG design are now chosen as parts of the B, C and D matrix of the standard plant.

5.2 Weighting functions and models

In the computation of the H_2 optimal controller, both G,H,W and E determine the shape of the optimal controller. Models for G and H were determined by means of identification techniques. The weighting functions W and E however are not obtained from modelling and specific decisions must be made. Choosing W and E makes the H_2 problem a nontrivial task, and an iterative procedure between weighing function selection and control design has to be used. After designing, an evaluation will take place and some adaptations will be made. For clarity, only the final design will be discussed.

The reason for adding the 2^{nd} order filter E before the output z_1 is taking the sensitivity of the ear for higher frequencies into account. This makes sense because the final goal is to reduce the inconvenience for people and not just reducing the noise level. The only problem with doing this is that the result has become more abstract. Something like the sense of hearing is more or less subjective.

Output z_2 will also be minimized to prevent the controller to give unconstrained control actions and become unstable. The 12^{th} order filter W consists of three components. The first is the inverse of the 8^{th} order model H. When looking at the closed loop transfer function there can be seen that this is done to compensate the closed loop effects.

$$W = \alpha \bar{W} H^{-1} \tag{5.5}$$

$$P_{cl,2} = \frac{HCW}{1+GC} = \frac{\alpha C \bar{W}}{1+GC} \tag{5.6}$$

The second component is the 4^{th} order filter $\bar{W}$. This is the part which does the real weighting. A form in the frequency domain is chosen linke a bathtub, in this way, only control in the interesting region is allowed. At low frequencies, no control action is desired because of the incapability of the speaker and microphone to work properly at these frequencies. The region where control activity is allowed must be wide enough to give the controller enough freedom. Before half the sample frequency, the controller has to drop off. $\bar{W}$ has two double poles at 40 and 1000 Hz. At last, W consist of the scaling factor α, which gives a variable to reduce or increase controller action.

The 8^{th} order transfer function H will also act as an weighting function. Therefore an exact representation of it is not necessary. The use of H is to indicate on what frequencies, it is most important to have a low sensitivity. Al magnitudes of the frequency responses of the interesting weighting functions are plotted in figure 5.2.

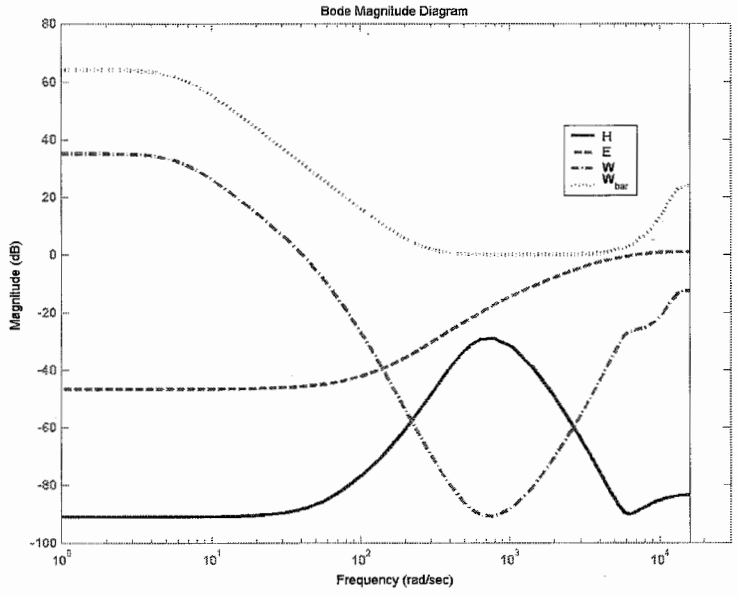

Figure 5.2: Weighting functions of the different processes

When the standard plant $P(q)$ is built up of the different components, a plant of order 50 is obtained. Because the weighting function $W(q)$ contains the inverse model $H(q)$, this weighing function has a high order and therefore increases the order of the plant $P(q)$. An alternative configuration without the inverse model of $H(q)$ is used. This plant no longer represents the physical system but gives the same 2-norm objective as used in equation 5.4. The new scheme will provide a 42^{th} order plant.

$$P(q) = \begin{bmatrix} HE & GHE \\ 0 & \alpha\bar{W} \\ 1 & G \end{bmatrix}, \quad P_{cl}(q,\theta) = \begin{bmatrix} \frac{HE}{1+CG} \\ \frac{HCW}{1+CG} \end{bmatrix} \tag{5.7}$$

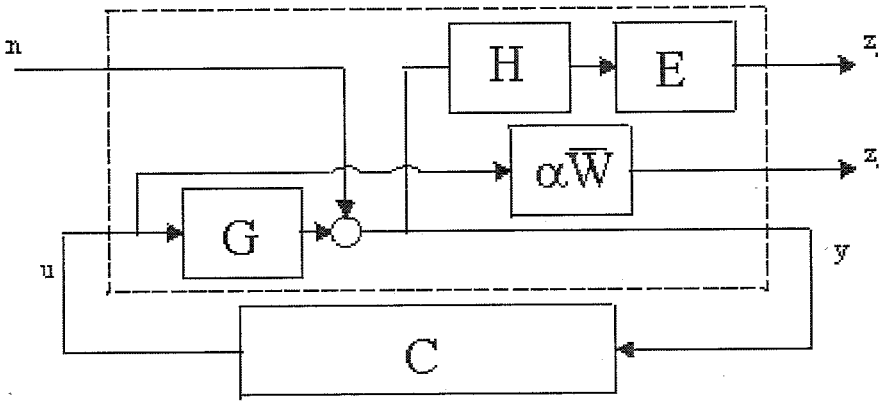

Figure 5.3: Alternative standard plant P

5.3 Results and analysis

The optimal 42^{th} order stable controller with system and weighing function describes as in the prior section is calculated. For the interpretation and analysis of the controller, a number of frequency responses has been plotted.

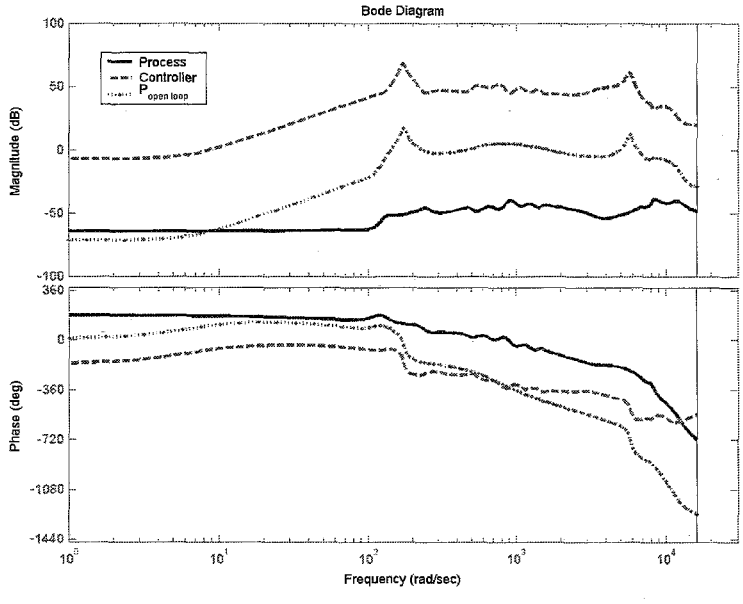

Figure 5.4: Open loop system

There can be seen that the controller will be active in the region from 20 to 1200 Hz. Below and above these frequencies, a decay of the controller is realized. There can be seen that the controller is quite strong and highly parameterized. The smooth open loop indicates a inversion of the process in some regions.

For the improvement in performance, the frequency response of performance qualifying transfer functions are plotted. In this figure the sensitivity of the ear is taken into account. This means that the output y is not used as an reference, but the output z_1 which is weighted with E to obtain an ear corrected sound level.

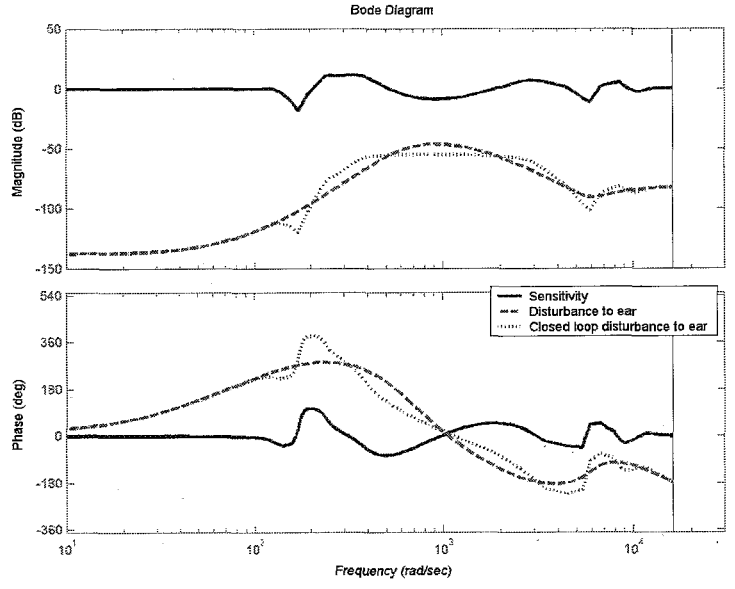

Figure 5.5: Sensitivity, uncontrolled and controlled disturbance

The sensitivity shows in what frequency ranges the noise is amplified or reduced. Clearly, in the region where the noise is most dominant, the closed loop noise is reduced. Just by looking at the bode plot, it is still hard to quantify the improvement. By dividing the open loop squared 2-norm and the closed loop squared 2-norm, a number is given to the performance improvement. This number also corresponds with the energy ratio.

$$\frac{\left\|\frac{HE}{1+GC}\right\|_2^2}{\|HE\|_2^2} = 0.3535 \tag{5.8}$$

The nyquist diagram of the open loop system gives a good impression of the stability margins.

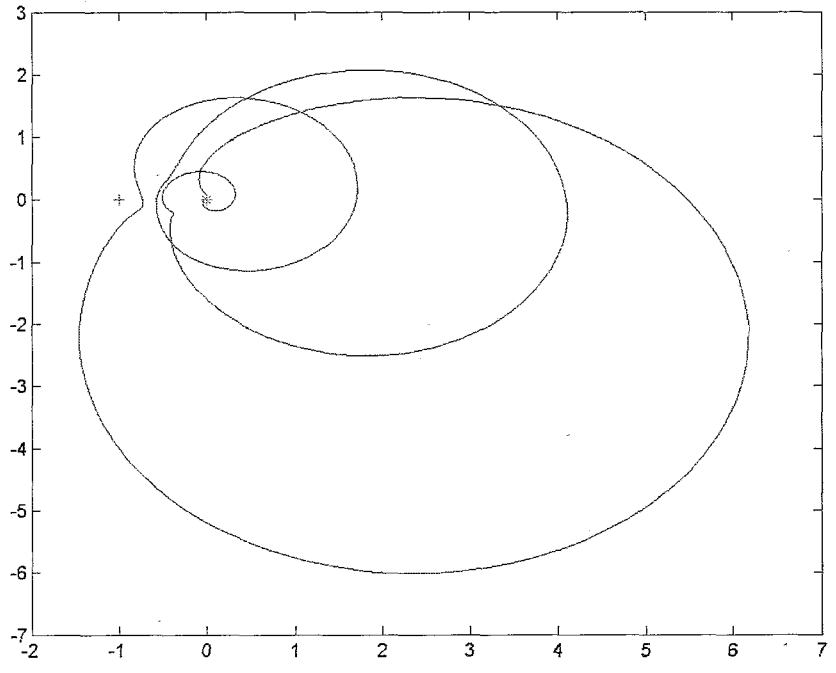

Figure 5.6: Nyquist diagram of the open loop system

When looking to the nyquist diagram, the big time shift attracts attention. The open loop figure is going in circles around the origin. It is clear that the big time delay in the system really limits its performance. The controller can amplify the gain at the moments the open loop frequency response is in the right half plane. In this way the sensitivity becomes below one. When the phase shifts in the direction of -180 degrees near the point -1, the controller has to reduce its gain. This is an explanation for the oscillating behavior of the controller.

Chapter 6

Controller reduction

In this chapter, controller order reduction will be handled. Simplifying the controller is favorable for implementation considerations. When reducing the controller, the behavior of the controller and the closed loop system will be changed. The performance of the closed loop system may suffer as little as possible because of the reduction. In equation 6.1, the difference in performance is stated in another form.

$$\left|\left|\frac{HE}{1+GC} - \frac{HE}{1+GC_{red}}\right|\right| = \left|\left|\frac{HE}{(1+GC)(1+GC_{red})}(C - Cred)\right|\right| \tag{6.1}$$

For a good reduction, weighted reduction should be applied, with a weighting as in equation 6.1. In this case is for simplicity reasons, chosen to weigh only with the sensitivity. Which is a part of the weighting in equation 6.1. One way to do this reduction is frequency weighted balanced truncation [8, Obinata], [9, Al-Saggaf].

6.1 Balanced realization truncation

First of all, the normal balanced realization truncation without weighing will be explained. The high order state space controller will be transformed to the balanced realization by the transformation matrix T.

$$\bar{x} = Tx \tag{6.2}$$

which transform the system to

$$\begin{aligned} \bar{x}(t+1) &= TAT^{-1}\bar{x}(t) + TBu(t) \\ y(t) &= CT^{-1}\bar{x}(t) \end{aligned} \tag{6.3}$$

A balanced realization means that the system will have equal and diagonal controllability and observability Gramians. This diagonal matrix is also sorted from high to low values.

$$\bar{W}_c = \bar{W}_o = diag(g) \tag{6.4}$$

The diagonal entries with the highest magnitude represent the states with the largest contribution to the output when the system is excited. In other words, the state vector is ordered in importance of contribution to responses caused by excitations at the input.

The reduction is quite simple now. When we have the balanced system

$$\begin{aligned} \bar{x}(t+1) &= \bar{A}\bar{x}(t) + \bar{B}u(t) \\ y(t) &= \bar{C}x(t) \end{aligned} \tag{6.5}$$

The system matrices can be decomposed as

$$\bar{A} = \begin{bmatrix} \bar{A}_{11} & \bar{A}_{12} \\ \bar{A}_{21} & \bar{A}_{22} \end{bmatrix}, \quad \bar{B} = \begin{bmatrix} \bar{B}_1 \\ \bar{B}_2 \end{bmatrix}, \quad \bar{C} = \begin{bmatrix} \bar{C}_1 & \bar{C}_2 \end{bmatrix} \tag{6.6}$$

The reduced system is created by truncation of the balanced system. Simply truncating the system does not guarantee stability any longer in the discrete time case. The property of the zero D-matrix which is important for control implementation keeps preserved.

$$\begin{aligned} x_r(t+1) &= \bar{A}_{11}x_r(t) + \bar{B}_1u(t) \\ y_r(t) &= \bar{C}_1x_r(t) \end{aligned} \tag{6.7}$$

6.2 Frequency weighted balanced truncation

With the understanding of balanced realization truncation, the weighing S can be added.

The state-variable realizations of C and S are given by:

$$C(q) = \left[\begin{array}{c|c} A_c & B_c \\ \hline C_c & 0 \end{array}\right], \quad S(q) = \left[\begin{array}{c|c} A_s & B_s \\ \hline C_s & D_s \end{array}\right] \tag{6.8}$$

It is not very hard to see that the state-variable realization of the product C and S is given by

$$C(q)S(q) = \left[\begin{array}{cc|c} A_c & B_cC_s & B_cD_s \\ 0 & A_s & B_s \\ \hline C_c & 0 & 0 \end{array}\right], \tag{6.9}$$

Frequency-weighted balanced truncation implies the balancing and truncations of those parts of the system and its state vector which are clearly associated with C.

6.3 Application to the controller

The controller has been reduced to a 14^{th} order controller by the frequency weighted balanced reduction. The sensitivity of the closed loop system with full order controller is used as weighing function. In this way, a good fit is obtained at the places where the sensitivity is high. A number of figures is plotted to compare the full order and the reduced order controller.

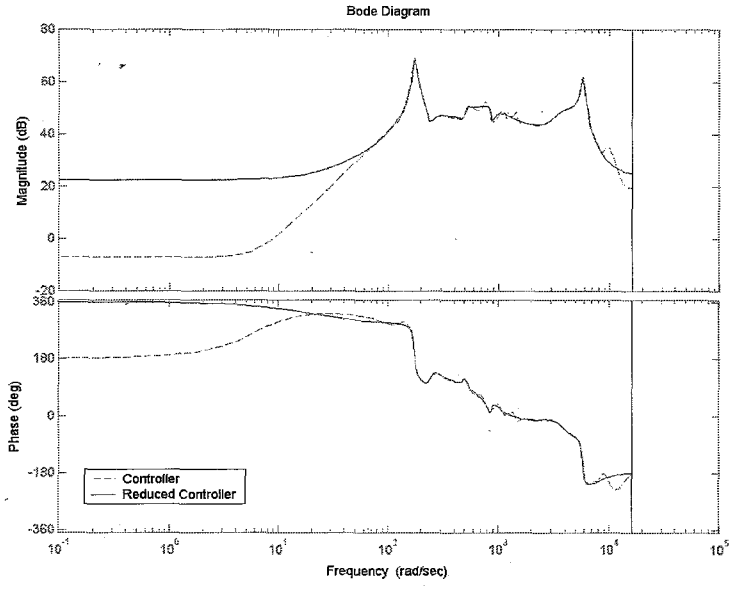

Figure 6.1: Bode figure of original and reduced controller

The reduced controller does not have the same DC-gain as the original controller. The property of the zero D-matrix however is maintained. This is because of reduction by truncation. A matching DC-gain is not important, as long as the DC-gain is low enough to have little control action at low frequencies. A zero D-matrix of the controller is required because a nonzero D-term can not be implemented. A nonzero D-term means that the controller has to sent a signal at the same moment, the signal comes in. In practice always one calculation step is needed.

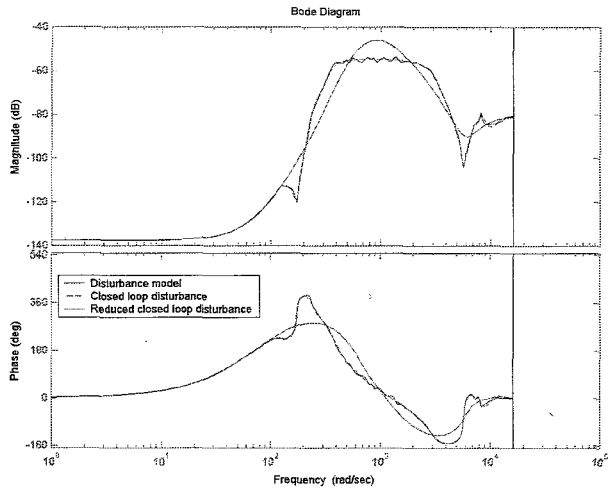

Figure 6.2: Open and closed loop disturbance with full and reduced order controller

The closed loop figure 6.2 shows clearly that the reduced controller almost gives the same performance as the full order controller. At the places where the amplitude of the closed loop disturbance is higher than the amplitude of the open loop disturbance is the sensitivity above one. At these places, the reduced closed loop disturbance resembles the full order closed loop disturbance in great detail. On other places, an oscillating line can be seen which is introduced by the reduction. At these places, there is no danger for instability.

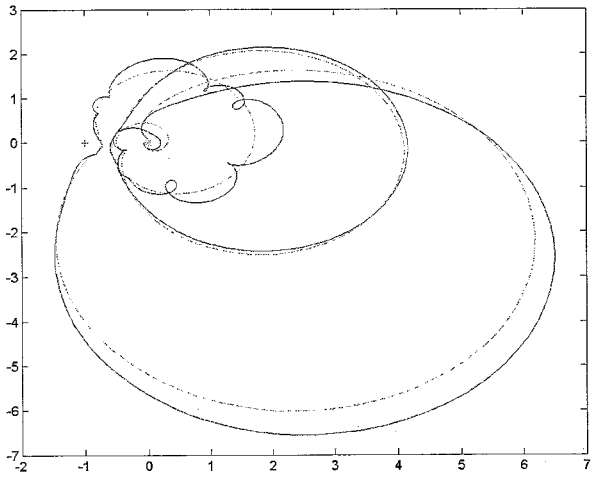

Figure 6.3: Nyquist diagram of open loop with full (dashed) and reduced order (solid) controller

Again, the nyquist figure confirms a good fit of the reduced an full order controller near the point -1. This gives an extra confidence about the stability of the reduced controller. The performance of the reduced controller closed loop system is also calculated.

$$\frac{\left\| \frac{HE}{1+GC_{red}} \right\|_2^2}{\|HE\|_2^2} = 0.3550 \tag{6.10}$$

When this is compared with the performance of the full order controller as calculated in equation 5.8, hardly any difference in performance is found. The reduction of the controller hardly affects the performance and does not cause any stability problems. It can be concluded that this reduction is successful and has maintained the desired closed loop performance of the ANC system.

Chapter 7

Implementation and validation

The 14^{th} order reduced state space controller is implemented at the designed sample frequency of 5.12 kHz. The performance of the ANC was less than expected. The reason for this is the AD-conversion before the controller. Especially because the gain of the process still increases at higher frequencies, aliasing is dominantly present.

A way to solve this, is adding an analog low-pass filter before the controller. The filter reduce the high frequent components so they will not be folded back at lower frequencies. The filter also alternates the dynamic behavior of the system. Especially the phase of the open loop system will decrease near the cutoff frequency. For that reason, the dynamic behavior of this filter is also added to the standard plant. In this way, an optimal controller can be calculated which gives an optimal noise reduction for the system including filter. Less performance can be reached for the system including the filter.

When the system including filter is implemented, an other problem will occur. The zero order hold at the end of the digital controller produces a staircase-form output signal. This output signal also contains higher harmonics of the original intended frequencies. The ear seems to be very sensitive for these higher harmonics, and the produced sound is just annoying. Again, this effect can be reduced by adding a low pass filter. This time between the controller and the speaker. This effect is tested by producing a pure sine wave by the controller. The unfiltered sound contains higher harmonics for which the ear is very sensitive. With the low pass filter added, these higher harmonics are removed, and mainly the pure sine wave will be heard. When implementing this second low pass filter, again a loss in performance will be made.

The two problems can be solved at once, just by using a higher sampling frequency. No new controller has to be calculated. The controller can be transformed to the frequency

domain by a zero order hold transformation and then be transformed back with the new sample frequency of 10.24 kHz. The high frequency controller will reduce its gain at higher frequencies and in the most important region, the same behavior is shown.

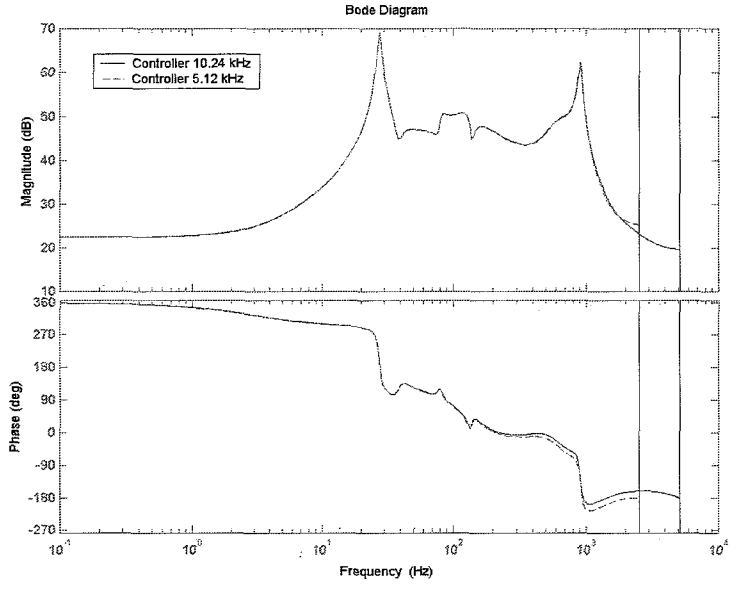

Figure 7.1: Reduced order and re-sampled reduced order controller

Frequency response data of the process G is used to check the closed loop behavior. The change in sample frequency does not cause any fundamental changes in closed loop behavior. At the higher frequency, the gain of the controller declines enough to prevent aliasing problems. Also the zero order hold operation now uses a higher sampling frequency which also places the higher harmonics at a higher frequency where the created disturbance is less dominant.

The controller is implemented and spectra of the uncontrolled and controlled error signals are measured. When these spectra are corrected for the sensitivity of the ear, they are compared.

In figure 7.2, the spectra of the uncontrolled and controlled ear sensitivity corrected error signal are depicted. The original spectra of the error signals are multiplied with the spectrum of the filter E. When these spectra are used to calculate the improvement of the closed loop system, the following improvement is found.

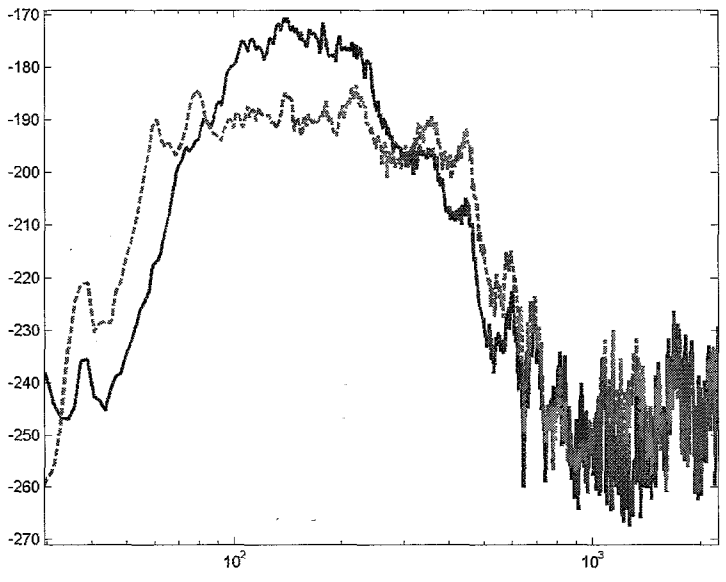

Figure 7.2: Power spectral density of the ear corrected noise of the open loop (solid) and closed loop (dashed) process

$$\frac{P_{e_{closed\ loop}}}{P_{e_{open\ loop}}} = \frac{\int_{-\pi}^{\pi} S_{e_{cl}}(\omega) S_{ear}(\omega) d\omega}{\int_{-\pi}^{\pi} S_{e_{ol}}(\omega) S_{ear}(\omega) d\omega} = 0.3877 \tag{7.1}$$

When this is compared with equation 6.10, almost the same result is obtained. The found controller satisfies the expectations and will not be alternated any more.

The obtained reduction is 61% in power. In systems involved with sound is the dB scale more common, this because of the logarithmic interpretation of sound. In those terms, a total sound reduction of 10 dB is achieved. This reduction is significant but not very high. Because of the large dimensions of the system, and then specifically the distance between the control speaker and the microphone, significant time delays are present. These reduce the performance drastically and makes only good control in the lower frequency ranges possible. In such an setup, feed forward control is more adequate [2]. However, when the dimensions of the system are smaller, feed forward control is often not feasible and feedback control as presented in this report is a powerful way to reduce noise.

Chapter 8

Proposal for alternative system setup

It showed that the time delay in the process G limits the noise reduction which can be obtained using feedback control. This time delay is caused by the time it takes for the sound to travel from the control speaker to the error microphone. A logic step would be to replace the speaker closer to the microphone or replacing the microphone closer to the speaker.

One problem this change in setup would create is the uncertainty if the noise measured at the microphone will still be of the same level as the noise leaving the duct. It can be expected that the noise can now be very well reduced at the location of the microphone, while the noise level at another point after the microphone will be higher. Therefore the next system configuration is proposed.

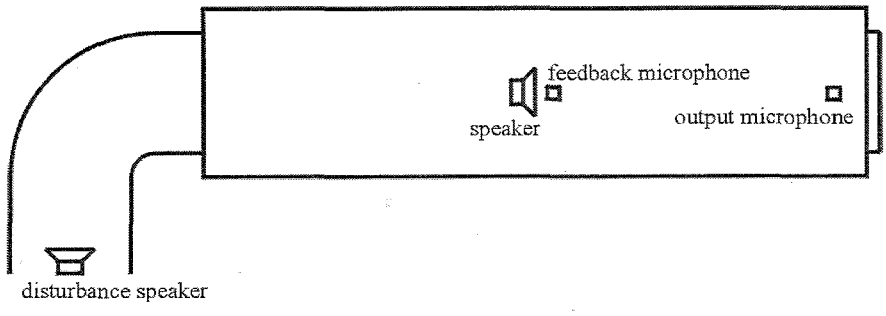

Figure 8.1: Alternative scheme of the silencer duct

In this setup, more processes are defined. G_1 relates the control input u and the output signal of the feedback microphone. G_2 relates the control input u and the output of the output microphone. The transfer function between the random white noise n and the

output of the feedback microphone is defined as H_1. And the transfer function between the noise n ant the output microphone is defined as H_2. With the definition of these processes, a standard plant can be formed as depicted in figure 8.2. However, the system will become more complex, there is expected that this setup will result in better noise suppression.

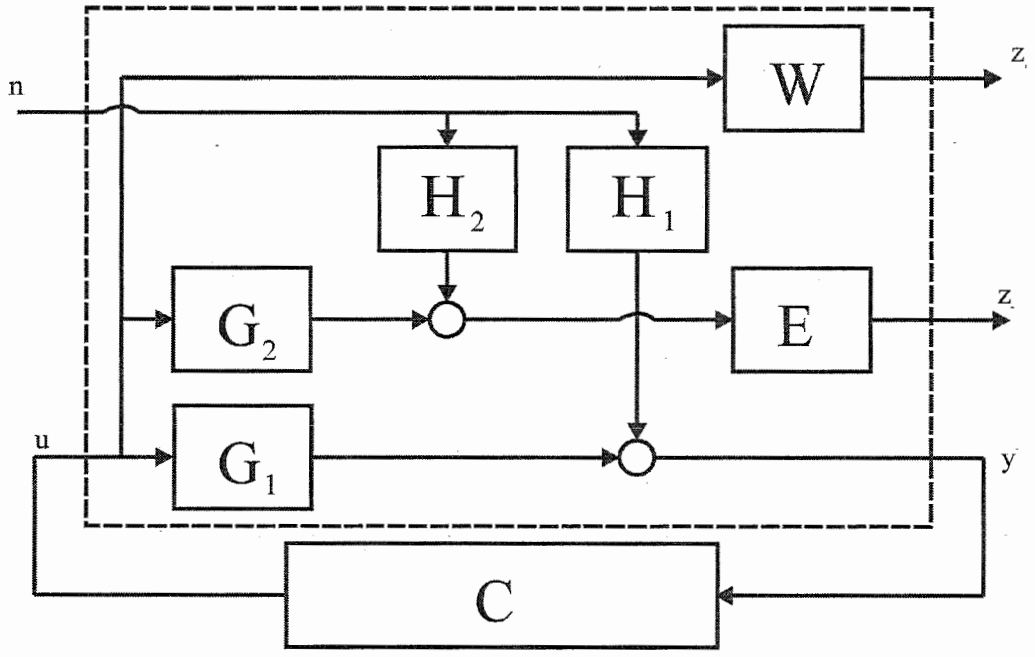

Figure 8.2: Standard plant with new configuration

Chapter 9

Conclusions

The acoustic duct is analyzed and models have been made. These models are combined to a standard plant with clear objective functions. The sensitivity of the ear is weighted in these objectives. A H_2 optimal noise reducing controller successfully has been designed. After implementation there is decided to run the controller at a higher sampling frequency of 10.24 kHz to avoid aliasing problems.

The final implemented controller reduces the ear corrected sound power to 39 percent of its original value. This corresponds with a reduction of 10 dB, which is a significant reduction. Because of the large distance between the control speaker and the microphone, time delays limit the control performance. For this particular system, better results can be obtained using feed-forward control. Nevertheless, when systems have smaller dimensions, very often no feed-forward control is possible, and feedback control can reduce noise at higher frequencies. This reports hands methods for an adequate feedback control solution for those systems.

Bibliography

[1] Wing Cheong Tang, Wei Zheng Lin, "Stiff light composite panels for duct noise reduction", *Applied Acoustics*, Vol. 64, pp. 511-524, 2003

[2] Jie Zeng, Raymond de Callafon, "Feedforward Noise Cancellation in an Airduct using Generalized FIR Filter Estimation", *Decision and Control, Proceedings*, Vol. 6 , pp. 6392 - 6397, Dec. 9-12, 2003

[3] A.J. Hull, C.J. Radcliffe, S.C. Southward, "Global active noise control of a one-dimensional acoustic duct using a feedback controller", *Journal of vibration and acoustics*, Vol. 115, pp. 488-494, sept. 1993

[4] Jeongho Hong, James C. Akers, Ravinder Venugopal, Miin-Nan Lee, Anderew G. Sparks, Peter D. Washabaugh, Dennis S. Bernstein, "Moddelling, Identification and Feedback Control of Noise in an Acoustic Duct", *IEEE Transactions on control systems technology*, vol. 4, no. 3, may 1996

[5] Lennart Ljung, *System identification: theory for the user*, Prentice Hall, Englewood Cliffs, New Jersey, 1987, ISBN: 0-13-881640-9

[6] Vasile Sima, *Algoritms for linear-quadratic optimization*, Marcel Dekker, New York, 1996, ISBN: 0-8247-9612-8

[7] Ali Saberi, Peddapullaiah Sannuti, Ben M. Chen, H_2 *optimal control*, Prentice Hall, London, 1995, ISBN: 0-13-489782-X

[8] Goro Obinata, Brian D.O. Anderson, *Model reduction for control system desing*, Springer, London, 2001, ISBN: 1-85233-371-5

[9] Ubaid M. Al-Saggaf, Gene F. Franklin, "Model reduction via balanced truncations: an extension and frequency weighting techniques", *IEEE trasaction on automatic control*, Vol. 33, No. 7, July 1988